Unrestricted slave-boson mean-field approximation for the two-dimensional Hubbard model

G. Seibold and E. Sigmund
Institut für Physik, Technische Universität Cottbus, PBox 101344, 03013 Cottbus, Germany

V. Hizhnyakov
Institute of Physics, Estonian Academy of Sciences, Riia 142, Tartu, Estonia

(Received 18 August 1997)

The Kotliar-Ruckenstein slave-boson scheme is used to allow for an unrestricted variation of the bosonic and fermionic fields on the saddle-point level. Various inhomogeneous solutions, such as spin polarons and domain walls, are discussed within the two-dimensional Hubbard model and compared with results of unrestricted Hartree-Fock (HF) calculations. We find that the present approach drastically reduces the polarization of these states and leads to increased delocalized wave functions as compared to the HF model. The interaction between two spin polarons turns out to be attractive over a wide range of the on-site repulsion U. In addition we obtain the crossover from vertical to diagonal domain walls at a higher value of U than predicted by HF. [S0163-1829(98)05807-X]

I. INTRODUCTION

The unrestricted Hartree-Fock (HF) approach has turned out to be a powerful tool in the calculation of inhomogeneous states in the Hubbard model.[1–6] Among them magnetic polarons,[1,8–11] domain walls,[2–5,7,29] and vortex solutions[6] have been extensively studied within the context of high-T_c superconductors (HTSC).

Schrieffer, Wen, and Zhang[8] have proposed the so-called spin-bag mechanism according to which a hole couples to the spin density of the antiferromagnetically (AF) ordered background of the CuO_2 planes, thus creating a local reduction of the AF order parameter. Within this model two holes are attracted by sharing a common bag. In the simplest model the resulting superconducting order parameter is of the order of the spin-density-wave gap, which is large enough to lead to high-temperature superconductivity. The concept of spin polaron formation is also successful in explaining the phase diagram in the low and intermediate doping regime of the HTSC's. According to the concept of microscopic electronic phase separation,[9,10] the doping-induced spin polarons (or spin clusters) form a conducting subsystem in a background dominated by strong antiferromagnetic correlations. Due to the competition between short-range attraction and the long-range Coulomb repulsion, these polarons do not form a homogeneous sea in an antiferromagnetic background. Instead, the holes are confined to a percolative network in which dimension D is lower than two ($1 \leqslant D \leqslant 2$). The resulting inhomogeneity in the electronic subsystem has also important implications on the pairing mechanism.[12]

Besides spin polarons, domain-wall solutions presently also attract a lot of interest in the field of HTSC. Stripe correlations have been observed in $La_{2-x}Sr_xCuO_4$,[13–15] in nickel oxide analogs of the copper oxides[16] and in $La_{1.6-x}Nd_{0.4}Sr_xCuO_4$.[17,18] In the two latter systems the density fluctuations are pinned by the underlying lattice structure giving rise to a static charge- and spin-density wave. The low-temperature orthorhombic phase in the nickel oxides stabilizes the stripe structure along the diagonals, whereas the low-temperature tetragonal structure in $La_{1.6-x}Nd_{0.4}Sr_xCuO_4$ favors the pinning of a horizontal stripe phase. Also in the CuO_2 planes of Bi2212 compounds the existence of charge stripe order has been demonstrated with extended x-ray-absorption fine structure (EXAFS) experiments.[19]

The stripe instability was predicted theoretically in Ref. 4 within a HF formalism applied to the extended Hubbard model. Also most of the further investigations on the striped phases[2,5,7,29] have been carried out within standard HF theory. However, the solutions obtained with HF are poor variational wave functions since they are much too high in energy. Within HF, the only mechanism avoiding double occupancy in order to reduce the Hubbard repulsion is to renormalize the spin-dependent on-site energy $\epsilon_{i,\sigma}=U\langle n_{i,-\sigma}\rangle$. Therefore the commensurate antiferromagnetic phase displays as an alternating shift of the spin-up and spin-down one-particle levels, respectively, which overestimates by far the polarization of the AF order.

It is well known that a part of the correlations between electrons of opposite spins can be accounted for by using the Gutzwiller projector.[21,22] For the AF ordered system this approach leads to wave functions that are very close in energy to the solution obtained by quantum Monte Carlo simulations.[23,24] In addition, the Gutzwiller wave function leads to a significantly lower spin polarization in the intermediate-U regime as compared to the HF result.[23] The Gutzwiller approach has also been used to improve the solutions of inhomogeneous states such as spin polarons[11,25] and domain walls.[25,26] However, due to computational limitations these calculations where done with an ansatz for the charge- and spin-density profile, i.e., the number of variational parameters for charge and spin at the different lattice sites has been strongly reduced.

In this paper we overcome the limitations discussed above and present results for unrestricted spin-polaronic and kink-type Gutzwiller wave functions. Our approach is based on the representation of the Hubbard model in terms of fermions and slave bosons due to Kotliar and Ruckenstein (KR).[27] The

 © 1998 The American Physical Society

KR formulation is a functional integral method that reproduces the Gutzwiller solution at the saddle-point level. The advantage of this method is that it provides a systematic way to improve the solution by expanding the fields around the saddle point. The KR approach is a good starting point for our purposes, since at the saddle-point level we can immediately identify the variational parameters with the bosonic and fermionic fields. Since we do not make any assumption on the spatial symmetry of these fields we therefore obtain various inhomogeneous textures in which stability depends on doping and the value of the Hubbard repulsion U. In the present paper we will concentrate on the stability and shape of spin-polaronic and domain-wall solutions, respectively. It turns out that for commensurate filling (i.e., one hole along the wall) the parameter range for the occurrence of stripes is significantly enlarged in comparison to the HF calculation. Within the investigated range of U ($4t \leqslant U \leqslant 10t$) we do not observe a crossover to a polaronic Wigner crystal for commensurate doping, which means that the interaction between the holes keeps attractive up to very large values of U.

The rest of the paper is organized as follows: In Sec. II we give a detailed description of the formalism, in Sec. III we present the results for spin polaronic and domain-wall solutions, respectively, and in Sec. IV we summarize our conclusions.

II. MODEL AND FORMALISM

We consider the two-dimensional Hubbard model on a square lattice, with hopping restricted to nearest neighbors (indicated by the bracket $\langle i,j \rangle$)

$$H = -t \sum_{\langle ij \rangle,\sigma} c^{\dagger}_{i,\sigma} c_{j,\sigma} + U \sum_{i} n_{i,\uparrow} n_{i,\downarrow}, \tag{1}$$

where $c^{(\dagger)}_{i,\sigma}$ destroys (creates) an electron with spin σ at site i, and $n_{i,\sigma} = c^{\dagger}_{i,\sigma} c_{i,\sigma}$. U is the on-site Hubbard repulsion and t the transfer parameter. For the calculations in Sec. III we take $t=1$. Following KR we enlarge the original Hilbert space by introducing four subsidiary boson fields $e^{(\dagger)}_i$, $s^{(\dagger)}_{i,\uparrow}$, $s^{(\dagger)}_{i,\downarrow}$, and $d^{(\dagger)}_i$ for each site i. These operators stand for the annihilation (creation) of empty, singly occupied states with spin up or down, and doubly occupied sites, respectively. Since there are only four possible states per site, these boson projection operators must satisfy the completeness condition

$$e^{\dagger}_i e_i + \sum_{\sigma} s^{\dagger}_{i,\sigma} s_{i,\sigma} + d^{\dagger}_i d_i = 1. \tag{2}$$

Furthermore

$$n_{i,\sigma} = s^{\dagger}_{i,\sigma} s_{i,\sigma} + d^{\dagger}_i d_i. \tag{3}$$

Then, in the physical subspace defined by Eqs. (2) and (3) the Hamiltonian (1) takes the form

$$\widetilde{H} = -t \sum_{\langle ij \rangle,\sigma} z^{\dagger}_{i,\sigma} c^{\dagger}_{i,\sigma} c_{j,\sigma} z_{j,\sigma} + U \sum_{i} d^{\dagger}_i d_i, \tag{4}$$

$$z_{i,\sigma} = \frac{1}{\sqrt{e^{\dagger}_i e_i + s^{\dagger}_{i,-\sigma} s_{i,-\sigma}}} (e^{\dagger}_i s_{i,\sigma} + s^{\dagger}_{i,-\sigma} d_i) \frac{1}{\sqrt{d^{\dagger}_i d_i + s^{\dagger}_{i,\sigma} s_{i,\sigma}}} \tag{5}$$

and has the same matrix elements as those calculated for Eq. (1) in the original Hilbert space.

In the saddle-point approximation, all bosonic operators are treated as numbers. The resulting effective one-particle Hamiltonian describes the dynamics of particles with modulated hopping amplitude and can be diagonalized by the transformation

$$c_{i,\sigma} = \sum_{k} \Phi_{i,\sigma}(k) a_k, \tag{6}$$

where the orthogonality of the transformation requires

$$\sum_{i,\sigma} \Phi^{*}_{i,\sigma}(k) \Phi_{i,\sigma}(q) = \delta_{kq}. \tag{7}$$

Given a system with N_{el} particles we finally obtain for the total energy

$$E_{\mathrm{tot}} = -t \sum_{\langle ij \rangle,\sigma} z^{*}_{i,\sigma} z_{j,\sigma} \sum_{k=1}^{N_{\mathrm{el}}} \Phi^{*}_{i,\sigma}(k) \Phi_{j,\sigma}(k) + U \sum_{i} d^{2}_i, \tag{8}$$

which has to be evaluated within the constraints (2), (3), and (7). This is achieved by adding these constraints quadratically to Eq. (8)

$$E_{C1} = \lambda_1 \sum_{i} \left(e^{2}_i + \sum_{\sigma} s^{2}_{i,\sigma} + d^{2}_i - 1 \right)^2, \tag{9a}$$

$$E_{C2} = \lambda_2 \sum_{i,\sigma} \left(\sum_{k} \Phi^{*}_{i,\sigma}(k) \Phi_{i,\sigma}(k) - s^{2}_{i,\sigma} - d^{2}_i \right)^2, \tag{9b}$$

$$E_{C3} = \lambda_3 \sum_{k,q} \left(\sum_{i,\sigma} \Phi^{*}_{i,\sigma}(k) \Phi_{i,\sigma}(q) - \delta_{kq} \right)^2, \tag{9c}$$

$$E_{C4} = \lambda_4 \left(\sum_{k,i} \Phi^{*}_{i,\uparrow}(k) \Phi_{i,\uparrow}(k) - N_{\uparrow} \right)^2, \tag{9d}$$

$$E_{C5} = \lambda_5 \left(\sum_{k,i} \Phi^{*}_{i,\downarrow}(k) \Phi_{i,\downarrow}(k) - N_{\downarrow} \right)^2. \tag{9e}$$

We have added the last two conditions that turn out to be very convenient because they allow one to define the total number of spin-up and -down particles $N_{\uparrow} + N_{\downarrow} = N_{\mathrm{el}}$. The energy functional $E\{\Phi_{i,\sigma}(k), e_i, s_{i,\sigma}, d_i\} = E_{\mathrm{tot}} + E_{C1} + E_{C2} + E_{C3} + E_{C4} + E_{C5}$ now has to be minimized with respect to the fermionic and bosonic fields. Since the KR theory does not preserve the spin-rotation invariance of the original Hamiltonian all variational parameters can be taken as real numbers.[28] For the minimization procedure we have used a standard conjugate gradient algorithm. The gradients of the functional $E\{\Phi_{i,\sigma}(k), e_i, s_{i,\sigma}, d_i\}$ can be calculated analytically and convergence is checked by evaluating the norm of the gradient. The accuracy of the solution can be controlled by calculating the value of $E_{C1} + E_{C2} + E_{C3} + E_{C4} + E_{C5}$ at the end of the iteration procedure. We generally have set the

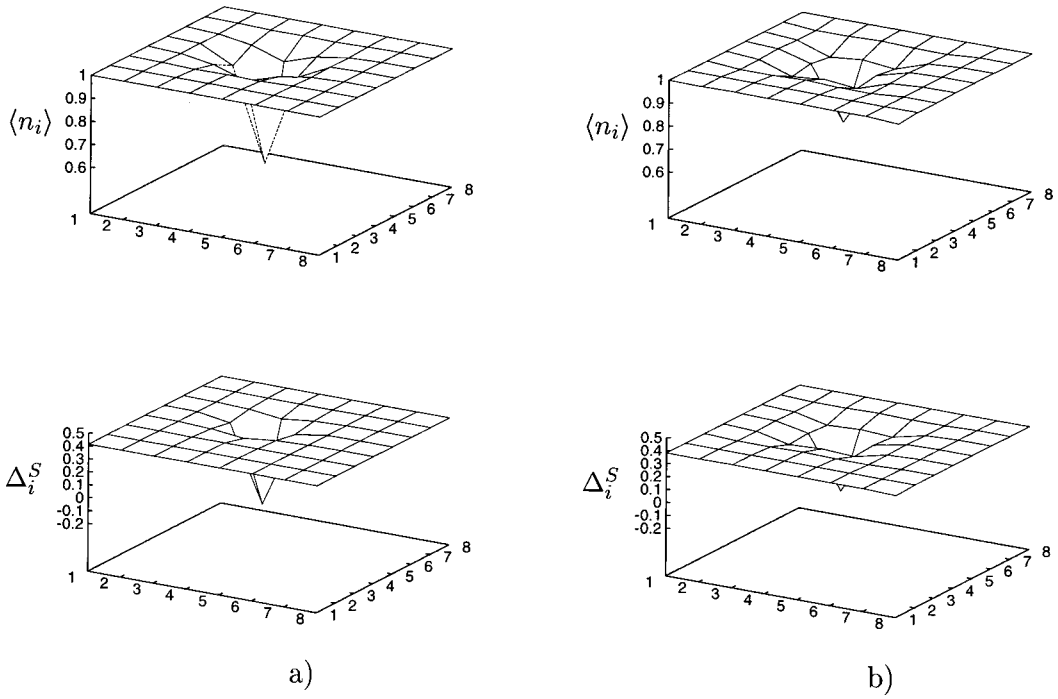

FIG. 1. Charge- ($\langle n_i \rangle$) and spin- (Δ_i^S) density profiles for a spin polaron on a 8×8 lattice. (a) HF approximation; (b) SB approximation. The Hubbard on-site repulsion is $U=6t$.

values of the Lagrange parameters $\lambda_1 \cdots \lambda_5$ to 10^4-10^5, which leads to an estimated error at ≈ 0.0002.

In principle one could start the calculation with a random configuration of the fermionic and bosonic fields. However, for a doped system there exist different self-consistent solutions that are close in energy and determining the most favorable can be difficult. Therefore, we have generally started from the unrestricted HF solutions for spin polaronic or domain-wall phases. The order of magnitude of the time needed to get convergence is half an hour on a SGI Indy workstation.

III. RESULTS

In a first step we consider a single spin polaron and compare the spin and charge profiles obtained within the HF and unrestricted slave-boson (SB) approximation, respectively. We then extend the calculations to domain-wall-type solutions and study the stability of these textures as a function of U. Before this, we evaluate the ground-state energy and AF polarization for the half-filled system and compare our calculations with the results of Yokoyama and Shiba.[23] Since for this case their AF Gutzwiller variational approach (AFGF) is equivalent to the saddle-point approximation of our slave-boson method we find perfect agreement within the numerical error. In contrast to the HF scheme, the AFGF leads to a significant reduction of the magnetization in the intermediate-U regime. On the other hand, both methods converge rapidly to fully polarized S_z components in the large-U limit. One should note that quantum Monte Carlo simulations[24] still lead to much smaller values in the large-U limit.

A. Spin polarons

The formation of spin polarons in the 2D Hubbard model results from the competition between kinetic energy gain and magnetic energy loss when doping the system away from half filling. Let us first consider the case where a particle with spin down has been removed from the half-filled, antiferromagnetically ordered lattice. If the vacancy is immobile, the cost in the magnetic energy is $4J \sim t^2/U$ in the large-U limit. However, this vacancy can gain kinetic energy via virtual hopping processes to the nearest-neighbor sites, thus mixing some probability of spin-up occupation to the site from where the particle has been removed. Therefore, the resulting spin-density profile therefore has an inverted order parameter at the site where the charge is located. According to Nagaoka's theorem[20] the size of this ferromagnetic core is expected to be very large for large values of U.

Figure 1 shows the charge- and spin-density profile of such a polaron obtained by unrestricted HF calculations and with the present method, respectively. The calculation was done on an 8×8 lattice with on-site repulsion $U=6t$. In both methods, the doped hole is mainly localized at site (4,5), but, whereas the charge at this site is reduced to $\langle n \rangle = 0.53$ within the HF approach, the unrestricted SB method gives a value of $\langle n \rangle = 0.73$ only. Moreover, the AF order parameter $\Delta_i^S = (-1)^{i_x+i_y} S_i^z$ at the polaron center is much less affected in the SB mean-field (MF) treatment ($\Delta_i^S = -0.07$) than in the case of unrestricted HF ($\Delta_i^S = -0.21$). This discrepancy can be understood as follows. The HF theory only renormalizes the spin dependent on-site energies. The removal of a spin-down particle at site i leads to a relaxation of the spin-up on-site level at this site. As a consequence the alternating on-site level shift, describing the AF

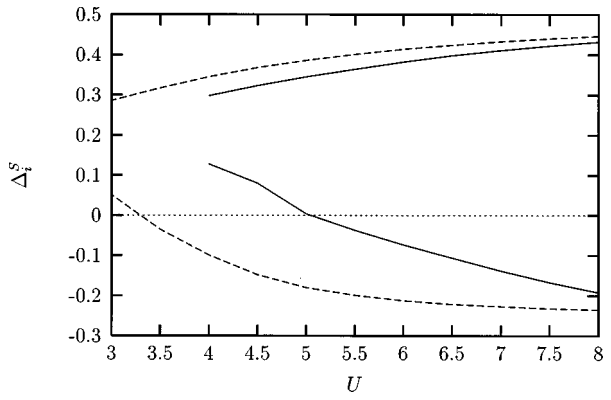

FIG. 2. Spin-density order parameter Δ_i^S at the center of the spin polaron (two lower curves) and at maximum distance from the polaron (two upper curves). Solid line: SB approximation; dashed line: HF approximation.

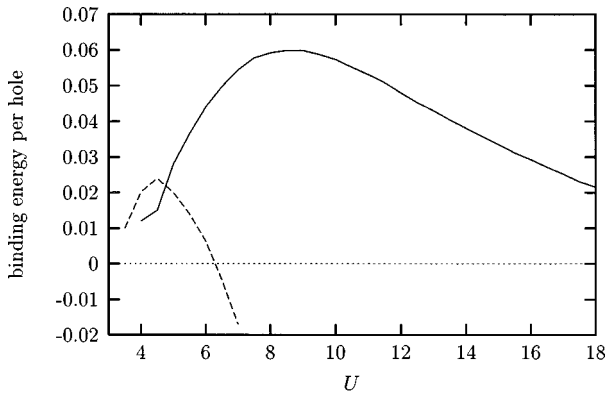

FIG. 3. Binding energy of a pair of polarons with opposite spins placed at neighboring sites on an 8×8 lattice. Dashed line: HF approximation; Solid line: SB approximation

order, is changed at site i where 5 neighboring spin-up states have now acquired nearly the same energy. Thus there is a strong hybridization between the spin-up states and one obtains a large value for the reversed spin order parameter at the central site i. By contrast the kinetic energy in the spin-down channel between site i and its nearest neighbors is very much reduced since the corresponding spin-down on-site level is pushed to a high energy. Note that the HF method always leads to a very large spin polarization, since this is the only way within this approximation to minimize the on-site repulsion.

Let us now consider the removal of a spin-down particle at site i when calculated within the SB aproximation. Then the spin-up hopping channel allows for the hybridization of neighboring spin up states with site i, which is comparable to the HF approach. However, since we now have an additional variational parameter per site (i.e., the boson field $\{d_i\}$) double occupancy can be minimized at site i, without greatly reducing the kinetic energy in the spin-down channel between site i and its nearest neighbors. In fact the reason the Gutzwiller wave function leads to a lower energy than HF theory is that there one can minimize double occupancy while keeping the kinetic energy at a higher value as compared to the HF approach. In other words, the localization behavior is much more pronounced in the HF treatment than within the SB formalism.

The energy difference of the solutions in Fig. 1 ($U=6t$) is of the same order of magnitude than for the homogeneous AF solutions of Ref. 23. The total energy per site calculated within the HF approximation is $E^{\mathrm{HF}}=-0.607t$ and for the SB method we get $E^{\mathrm{SB}}=-0.645t$. Figure 2 shows the order parameter Δ_i^S as a function of U at the perturbed sites and far from the spin polaron, evaluated with HF and SB approximations, respectively. It turns out that the SB method drastically reduces the polarization at the center of the polaron as compared to HF. As can be further seen on Fig. 2, this reduction of polarization is much stronger than in the residual AF ordered plane. Within the SB scheme the spin polaron acquires a ferromagnetic core for values $U>5t$ whereas this limit in HF is already achieved for $U\approx3.3t$.

Finally we evaluate the static interaction between two spin polarons, which is of special importance with regard to the spin-bag model[8] and phase separation scenarios[9] of the high-T_c superconductors. To calculate the binding energy we consider two holes with opposite spins placed at two neighboring sites and compare the energy of this configuration with the energy of two infinitely separated spin polarons. It should be noted that a positive binding energy means attraction. The results are plotted in Fig. 3. Within the HF approach we obtain an interaction between the two polarons that is attractive up to $U\approx6.5t$, in agreement with the results of Ref. 1. The binding energy displays a maximum at $U\approx4.5t$. However, within the SB approximation the parameter space of attraction is considerably enlarged. The maximum of the binding energy, which is approximately twice the value of the HF calculation, now occurs at $U\approx8.5t$. Unfortunately, convergence of our variational approach becomes very slow in the very large-U regime. In this limit one has to greatly increase the parameters λ_i in Eq. (9) in order to keep the constraint-induced error within the desired limits. This fact causes the difficulty in exploring the whole parameter range of attraction in Fig. 3.

B. Domain-wall solutions

For intermediate values of the on-site Hubbard repulsion U Hartree-Fock theory predicts the existence of domain-wall solutions, where the doped charged carriers are localized within a stripe in horizontal or diagonal direction. This stripe separates two AF ordered regions with opposite sign in the AF order parameter. Within the HF approximation it was shown[5] that there is a transition from horizontal to diagonal stripes when the ratio between on-site repulsion U and transfer integral t exceeds the critical value of $U/t\approx3.6$. From a constrained Gutzwiller variation of hyperbolic-type domain walls it was concluded in Ref. 26 that this limit probably is shifted to much lower values.

In the following we will compare energies for diagonal and horizontal stripes with the energy of isolated spin polarons using the unrestricted SB scheme. The calculations are made for different lattice sizes (typically 17×4, 13×6, 9×8) by applying appropriate boundary conditions for each domain wall type (see Fig. 4). The choice of the supercell is, of course, a delicate issue since periodic boundary conditions in principle require an ''uneven $\times$ uneven'' lattice for a diagonal wall and an ''uneven $\times$ even'' lattice for a vertical

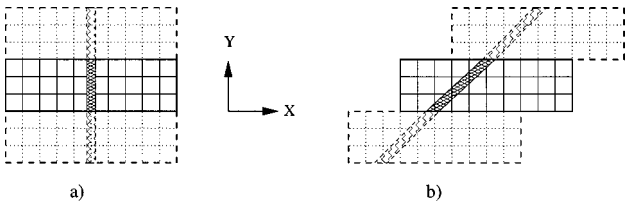

FIG. 4. Sketch showing the boundary conditions in the y direction, which have been applied to describe vertical (a) and diagonal (b) domain walls, respectively. In the x direction we have taken periodic conditions. The line crossings correspond to the lattice sites and the dashed lattices mark the chosen periodicity in the y direction.

stripe. To avoid the comparison between different lattice sizes for different domain wall types we have chosen the ''shifted boundaries'' shown in Fig. 4(b). This means that along the y direction the supercells are shifted by the extent of the diagonal domain wall in x direction. Consider, for example, a diagonal domain wall on a 13×6 lattice. Then the site $(N_x,1)$ is connected with site $(N_x+6,6)$ for $N_x<8$ and with site $(N_x+6-13,6)$ for $N_x\geqslant8$. Calculating the energy per site for the half-filled AF ordered system, we find that the two kinds of boundary conditions in Fig. 4 differ in the result by 0.1% for $U\approx3t$. This difference rapidly vanishes with increasing U.

In Fig. 5 we show the charge- and spin-density profile of a vertical domain wall calculated with unrestricted HF and SB approximations, respectively. The doping corresponds to one hole per site in the domain wall. As for the spin polarons studied in the previous section the SB result displays a charge- and spin profile that is considerably enlarged compared to the HF solution. This is in agreement with the calculations of Ref. 26. The dip in the HF charge profile is nearly twice the value of the SB approximation.

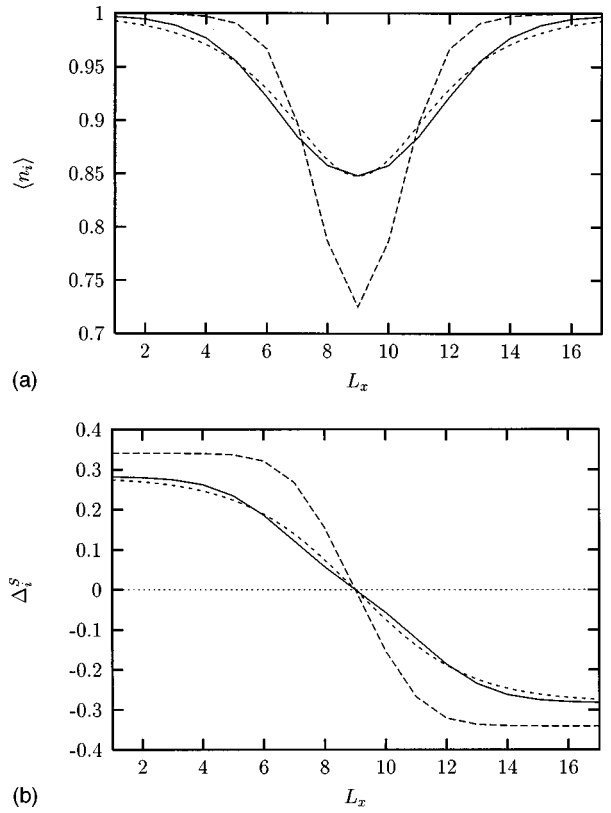

FIG. 5. Charge- (a) and spin- (b) density profiles in the x direction for a vertical domain wall on a 17×4 lattice. The number of holes is 4 since the best energy is obtained when there is one hole per site in the wall. Solid lines: SB approximation; dashed lines: HF approximation; short dashed: cosh (for charge) and tanh (for spin) functional fit to the SB solution.

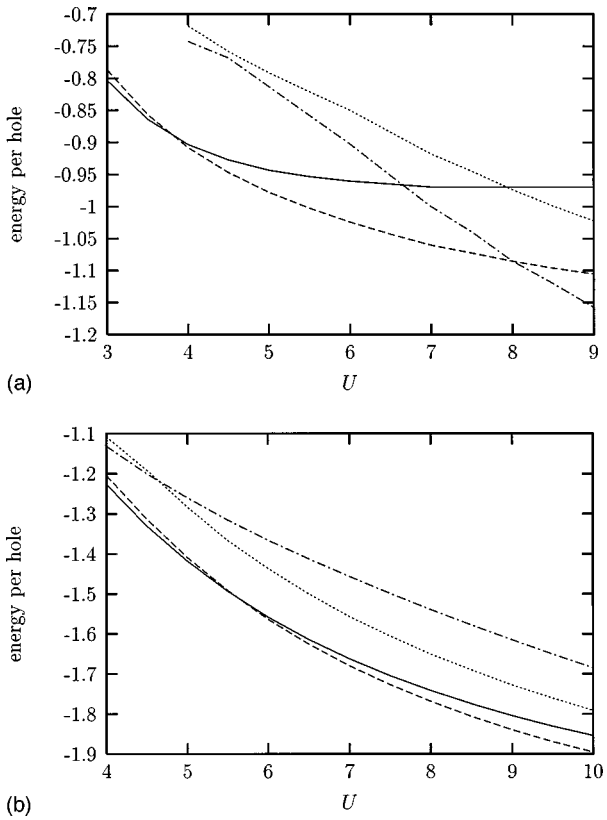

FIG. 6. Binding energy per hole for vertical stripes (full lines), and diagonal stripes (dashed lines) with one hole per site along the wall, vertical half-filled walls (dotted lines) and isolated spin polarons (dashed-dotted lines). The binding energy is defined as the difference in energy between a given texture and the homogeneous AF ordered lattice with the same doping. The domain wall solutions have been calculated on a 9×8 lattice, polarons on a 8×8 lattice. (a) HF approach; (b) SB approximation.

Figure 6 shows the energy per hole as a function of U for various textures such as domain walls and spin polarons. We also have investigated the half-filled wall with the on-wall quadrupling of the period, which has been intensively discussed by Zaanen and Oleś in Ref. 29. The energy has been calculated in a standard way[29] by comparing the energy of each texture with the energy of the homogeneous AF ordered state with the same number of holes (compared to half filling). In the case of the diagonal wall we additionally have chosen the same shift of the boundaries for the reference AF lattice.

Within the HF approximation we obtain a crossover from vertical to diagonal domain walls for $U\approx3.8t$ and a crossover to isolated spin polarons at $U\approx8t$. The energy for half-filled walls is always higher than for isolated polarons. These results are in complete agreement with earlier HF studies of the two-dimensional Hubbard model.[5,29] However, the range

of stability for the vertical stripe solution is considerably enlarged in the unrestricted SB approximation where we obtain the crossover at $U \approx 5.7t$. This result is supported by Lancos diagonalization studies of the t-J model[30] and Monte Carlo methods of the one-band Hubbard model.[31–33] These works report a shift of the static spin structure factor peak in the vertical direction when the charge density is reduced away from half filling in agreement with our findings. Also recent studies of the 2D t-J model within a density-matrix renormalization-group approach[34] are in agreement with a vertical striped phase. In addition we do not observe a crossover to a spin-polaronic Wigner crystal for the considered range of U ($U \leqslant 10t$). Instead the energy of half-filled walls turns out to be lower than the energy of spin polarons. In fact, since in the SB approach the range of attraction between the holes is considerably enhanced, these textures are energetically favored, which has the holes placed nearby each other. However, for very large values of U we again expect a decay of the stripe into isolated polarons.

IV. CONCLUSIONS

We have shown that the unrestricted SB saddle-point approximation is a simple and powerful tool to improve inhomogeneous solutions obtained by the HF method. It turns out that this approach leads to a strong reduction of the spin polarization of these inhomogeneities in the intermediate-U regime. The most relevant feature of the SB approximation, however, is the considerably enlarged range of attraction between spin polarons in comparison with the HF method. This result has also a strong impact on the spin-bag model of high-T_c superconductivity, since HF theory has restricted the validity of this model to small values of the Hubbard repulsion U.

Regarding the domain-wall phases, we find that the crossover from vertical to horizontal stripes is shifted to higher values of the on-site repulsion U than predicted by HF theory. Moreover we do not observe a crossover to isolated polarons for $U \leqslant 10t$. This result supports the description of domain-wall structures in the La_2NiO_4 compounds[35] where it is generally argued that the occurrence of diagonal walls is a result of mean-field theory. Within the present approach the range of stability of diagonal walls is considerably enhanced in comparison to the HF approximation, where for $U \approx 8t$ the walls decay into isolated polarons.

ACKNOWLEDGMENTS

Valuable discussions with W. Essl are gratefully acknowledged. We also thank A. Bill for a critical reading of the manuscript.

[1] W. P. Su and X. Y. Chen, Phys. Rev. B **38**, 8879 (1988).
[2] D. Poilblanc and T. M. Rice, Phys. Rev. B **39**, 9749 (1989).
[3] H. J. Schulz, J. Phys. (France) **50**, 2833 (1989).
[4] J. Zaanen and O. Gunnarsson, Phys. Rev. B **40**, 7391 (1989).
[5] M. Inui and P. B. Littlewood, Phys. Rev. B **44**, 4415 (1991).
[6] J. A. Vergés, E. Louis, P. S. Lomdahl, F. Guinea, and A. R. Bishop, Phys. Rev. B **43**, 6099 (1991).
[7] H. J. Schulz, Phys. Rev. Lett. **64**, 1445 (1990).
[8] J. R. Schrieffer, X.-G. Wen, and S.-C. Zhang, Phys. Rev. Lett. **60**, 944 (1988).
[9] V. Hizhnyakov and E. Sigmund, Physica C **16**, 655 (1988); V. Hizhnyakov, N. Kristoffel, and E. Sigmund, Physica C **161**, 435 (1989); **160**, 119 (1989); V. Hizhnyakov, E. Sigmund, and M. Schneider, Phys. Rev. B **44**, 795 (1991).
[10] V. Hizhnyakov, E. Sigmund, and G. Seibold, in *Proceedings of the 1st Workshop on Phase Separation in Cuprate Superconductors, Erice, 1992*, edited by K. A. Müller and G. Benedek (World Scientific, Singapore, 1993).
[11] G. Seibold, E. Sigmund, and V. Hizhnyakov, Phys. Rev. B **48**, 7537 (1993).
[12] V. Hizhnyakov and E. Sigmund, Phys. Rev. B **53**, 5163 (1996); E. Sigmund, V. Hizhnyakov, and A. Bill, Z. Phys. Chem. (Munich) **201**, 245 (1997).
[13] S.-W. Cheong, G. Aeppli, T. E. Mason, H. Mook, S. M. Hayden, P. C. Canfield, Z. Fisk, K. N. Clausen, and J. L. Martinez, Phys. Rev. Lett. **67**, 1791 (1991).
[14] T. E. Mason, G. Aeppli, and H. A. Mook, Phys. Rev. Lett. **68**, 1414 (1992).
[15] T. R. Thurston, P. M. Gehring, G. Shirane, R. J. Birgeneau, M. A. Kastner, Y. Endoh, M. Matsuda, K. Yamada, H. Kojima, and I. Tanaka, Phys. Rev. B **46**, 9128 (1992).
[16] J. M. Tranquada, D. J. Buttrey, V. Sachan, and J. E. Lorenzo, Phys. Rev. Lett. **73**, 1003 (1994).
[17] J. M. Tranquada, J. D. Axe, N. Ichikawa, Y. Nakamura, S. Uchida, and B. Machumi, Phys. Rev. B **54**, 7489 (1996).
[18] J. M. Tranquada, J. D. Axe, N. Ichikawa, A. R. Moodenbaugh, Y. Nakamura, and S. Uchida, Phys. Rev. Lett. **78**, 338 (1997).
[19] A. Bianconi, N. L. Saini, A. Lanzara, M. Missori, T. Rossetti, H. Oyanagi, H. Yamaguchi, K. Oka, and T. Ito, Phys. Rev. Lett. **76**, 3412 (1996).
[20] Y. Nagaoka, Phys. Rev. **147**, 392 (1966).
[21] M. C. Gutzwiller, Phys. Rev. Lett. **10**, 159 (1963).
[22] M. C. Gutzwiller, Phys. Rev. **137**, A1726 (1965).
[23] H. Yokoyama and H. Shiba, J. Phys. Soc. Jpn. **56**, 3582 (1987).
[24] J. E. Hirsch, Phys. Rev. B **31**, 4403 (1985).
[25] S. N. Coppersmith and Clare C. Yu, Phys. Rev. B **39**, 11 464 (1989).
[26] T. Giamarchi and C. Lhuillier, Phys. Rev. B **42**, 10 641 (1990).
[27] G. Kotliar and A. E. Ruckenstein, Phys. Rev. Lett. **57**, 1362 (1986).
[28] In HF theory this corresponds to setting the spin-flip expectation values $\langle c_\sigma^\dagger c_{-\sigma} \rangle = 0$.
[29] J. Zaanen and M. Oleś, Ann. Phys. (Leipzig) **5**, 224 (1996).
[30] A. Moreo and E. Dagotto, Phys. Rev. B **42**, 4786 (1990).
[31] A. Moreo, D. J. Scalapino, R. Sugar, S. White, and N. Bickers, Phys. Rev. B **41**, 2313 (1990).
[32] M. Imada and Y. Hatsugai, J. Phys. Soc. Jpn. **60**, 3752 (1989).
[33] N. Furukawa and M. Imada, J. Phys. Soc. Jpn. **61**, 3331 (1992).
[34] S. R. White and D. J. Scalapino, e-print cond-mat/9705128.
[35] J. Zaanen and P. B. Littlewood, Phys. Rev. B **50**, 7222 (1994).